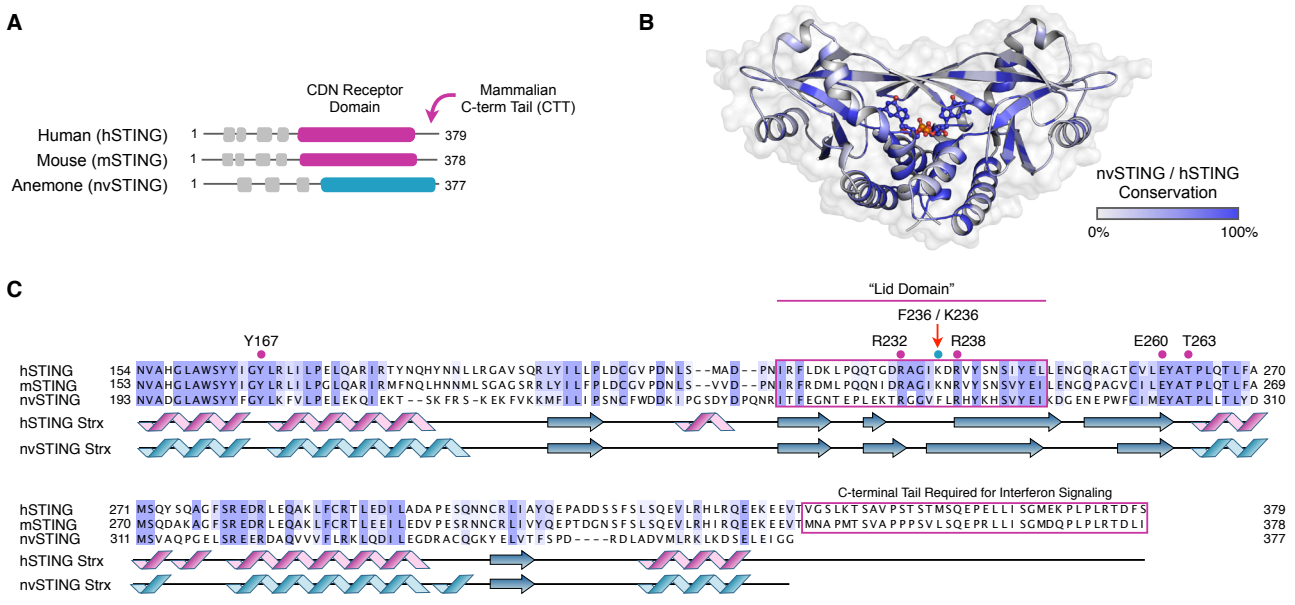

Figure S1. nvSTING and hSTING Alignment, Related to Figure 1

(A) Cartoon schematic of human, mouse and anemone STING proteins. Predicted transmembrane domains are indicated in grey, and the crystallized CDN receptor domain is indicated in magenta or blue. (B) Structure of nvSTING–3′,3′ cGG colored according to phylogenetic amino-acid conservation. (C) Detailed sequence alignment of human, mouse and anemone CDN receptor domains colored according to phylogenetic conservation. Known hSTING and nvSTING secondary structures are depicted below (α-helices in magenta / blue, and β-strands in dark blue arrows). Ligand interacting residues are indicated, as well as the beta-strand lid domain and the unique mammalian carboxy-terminal tail required for modern interferon signaling.

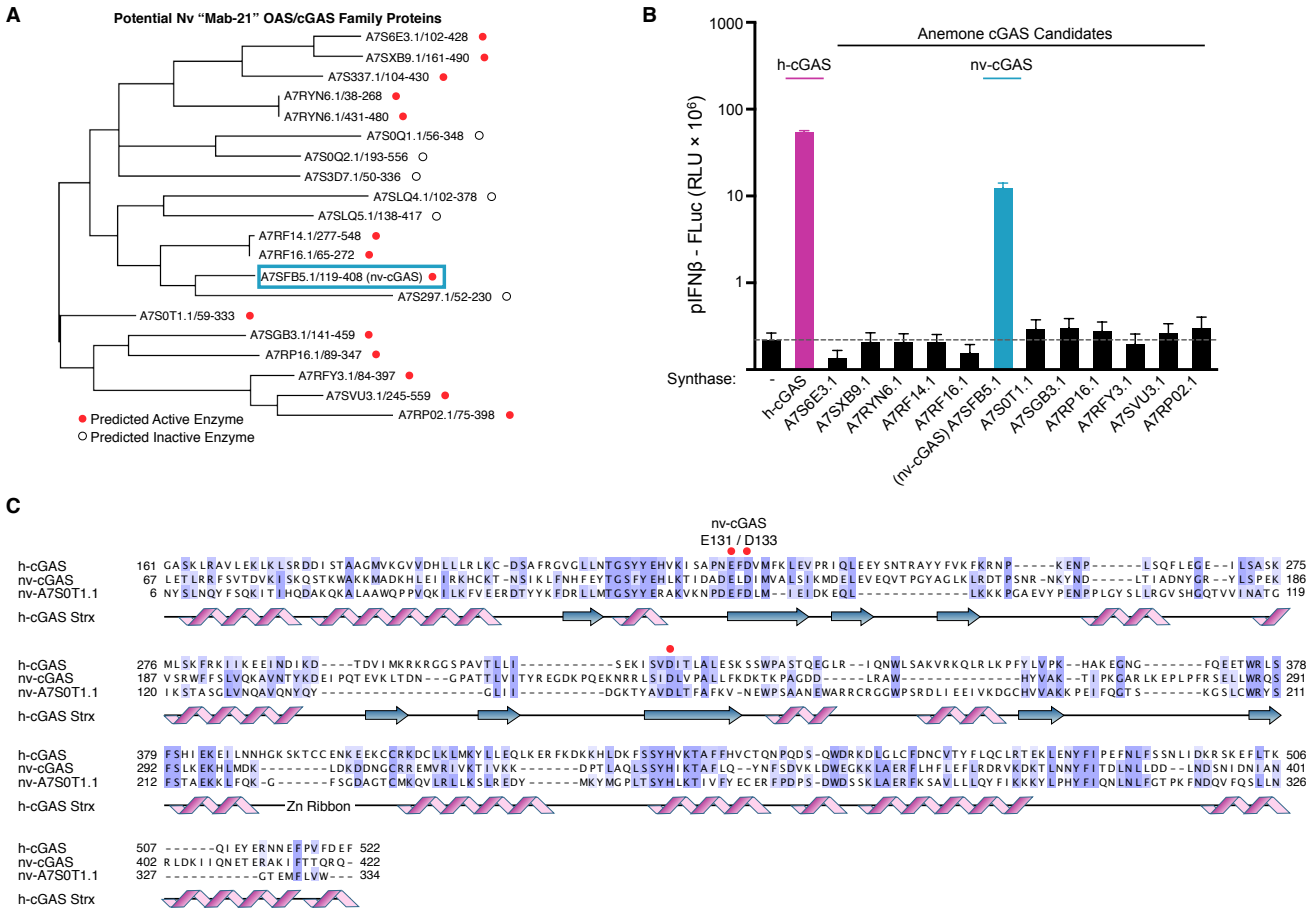

Figure S2. Cellular-Based Screen Identifying nv-cGAS, Related to Figure 2

(A) Phylogenetic alignment of all potential "Mab-21" OAS/cGAS family proteins. Potential candidate synthases with a predicted catalytic active site based on alignment to human cGAS are denoted (red circle), as well as predicted inactive enzymes (white circle). (B) Screen for CDN synthase activity using interferon β assay as in Figure 2A. Positive activity is only detected with gene nv-cGAS (nv-A7SFB5.1), and not any other related candidate anemone gene. (C) Detailed sequence alignment of synthase domains from human cGAS, nv-cGAS (nv-A7SFB5.1), and related candidate synthase nv-A7S0T1.1. Alignment is colored according to phylogenetic conservation, and a red circle denotes human cGAS active-site residues. Position of the nv-cGAS E131A/D133A mutation in Figure 2 is indicated.

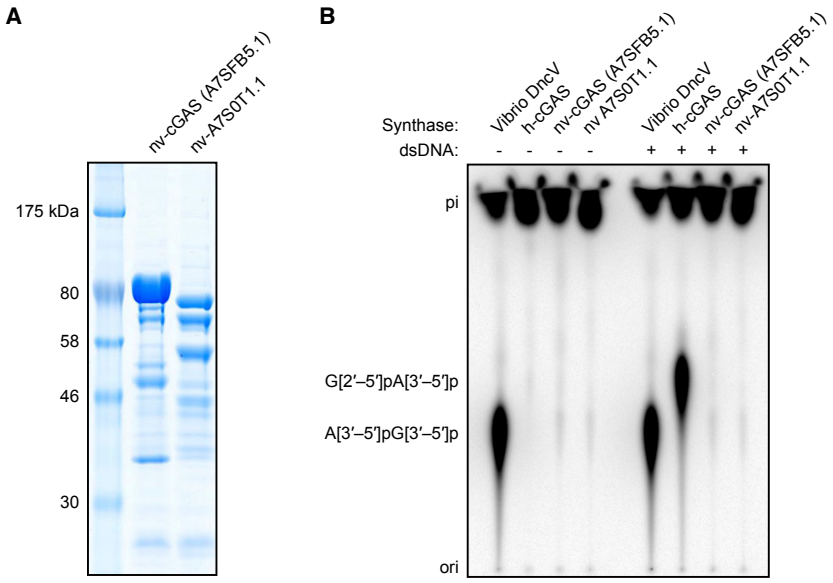

Figure S3. Nv-cGAS Activity is Not Stimulated by dsDNA, Related to Figure 2
(A) SDS-PAGE analysis of recombinant nv-cGAS and nv-A7S0T1.1 protein purified as MBP-fusion proteins expressed in E. coli. (B) In vitro analysis of Vibrio DncV, human cGAS, nv-cGAS and nv-A7S0T1.1 CDN product formation. Reactions were labeled with α-^{32}P GTP and include dsDNA stimulation as indicated. Subsequently, reactions were treated with alkaline phosphatase and separated by thin layer chromatography. Vibrio DncV constitutively produces 3′,3′ cGAMP, while human cGAS only produces 2′,3′ cGAMP in the presence of activating dsDNA. No CDN product is detected for nv-cGAS enzyme in either condition, suggesting that a different ligand may be required for nv-cGAS activation. Image is representative of multiple independent experiments, and identical results were observed with α-^{32}P ATP.

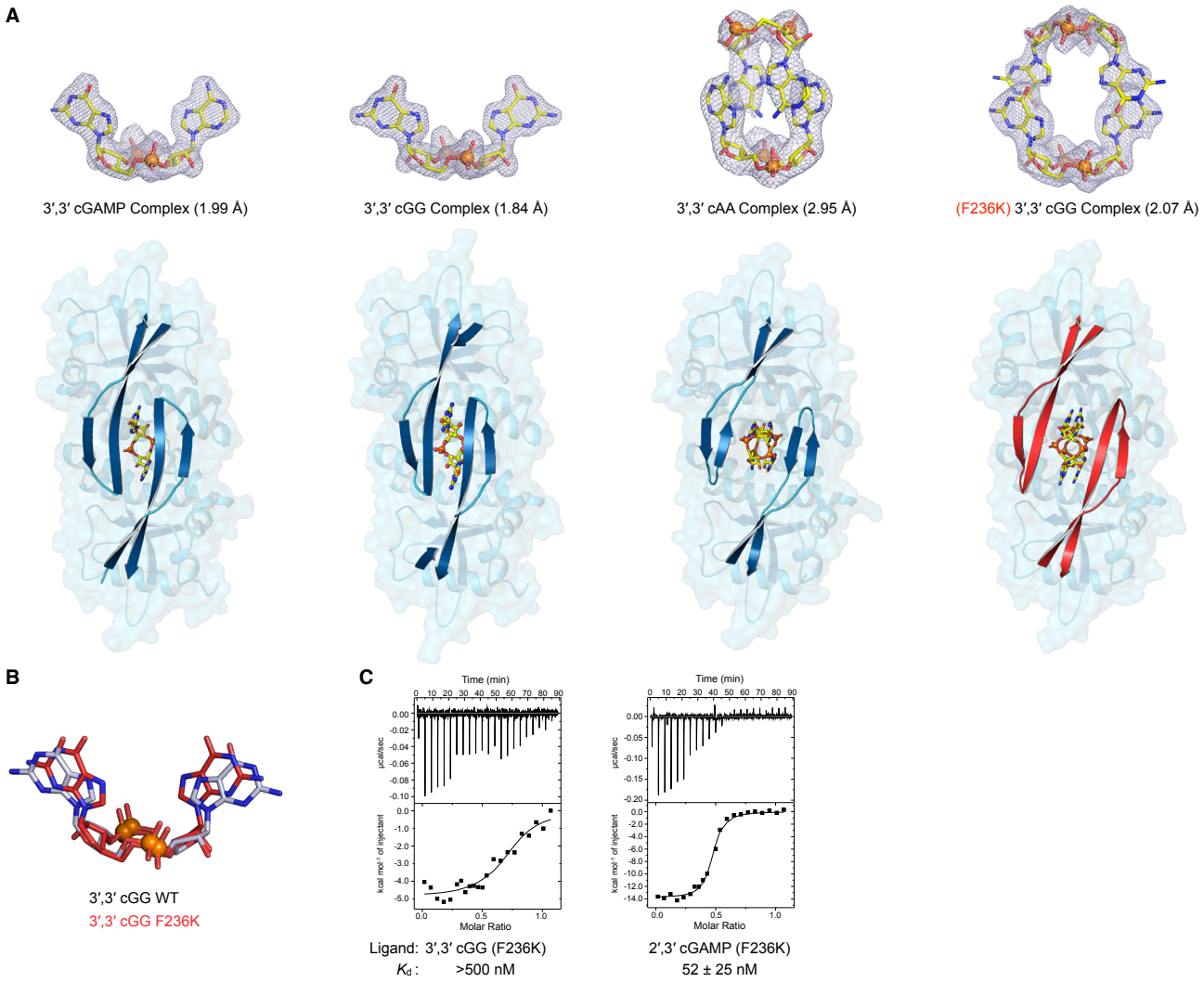

Figure S4. nvSTING 3′,3′ Sequence-Specific Lid Closure, Related to Figures 3 and 4

(A) $2F_o-F_c$ maps of nvSTING-bound 3′,3′ cyclic-dinucleotide ligands (contoured to 1.5 σ) and top-down view of nvSTING-bound crystal structures with highlighted beta-strand lid domains. 3′,3′ cGAMP and 3′,3′ cGG induce tight lid domain closure, while 3′,3′ cAA is unable to induce lid closure. The open lid domain allows room for a second 3′,3′ cAA molecule to slip-stack between the bound 3′,3′ cAA ligand, a crystallization effect observed previously in other crystal structures of CDN binding proteins (Sureka et al., 2014). The humanizing F236K mutation (actual nvSTING amino acid position F276) in nvSTING results in an open lid conformation (red) even when bound to 3′,3′ cGG. The open nvSTING(F236K)–3′,3′ cGG lid domain adopts an identical conformation as the nvSTING–3′,3′ cAA lid domain and allows a second 3′,3′ cGG molecule to slip-stack between the bound ligand. (B) Cartoon representation of the high affinity nvSTING–3′,3′ cGG bound ligand compared to the loosely organized nvSTING(F236K)–3′,3′ cGG ligand, which adopts a conformation identical to nvSTING–3′,3′ cAA. (C) ITC measurements of nvSTING(F236K) affinity for 3′,3′ cGG and 2′,3′ cGAMP ligands, as indicated. The humanizing mutation reduces high-affinity 3′,3′ cGG interactions while still allowing the intermediate STING conformation to form a high-affinity complex with 2′,3′ cGAMP. ITC data is representative of independent experiments. See also Table S1.

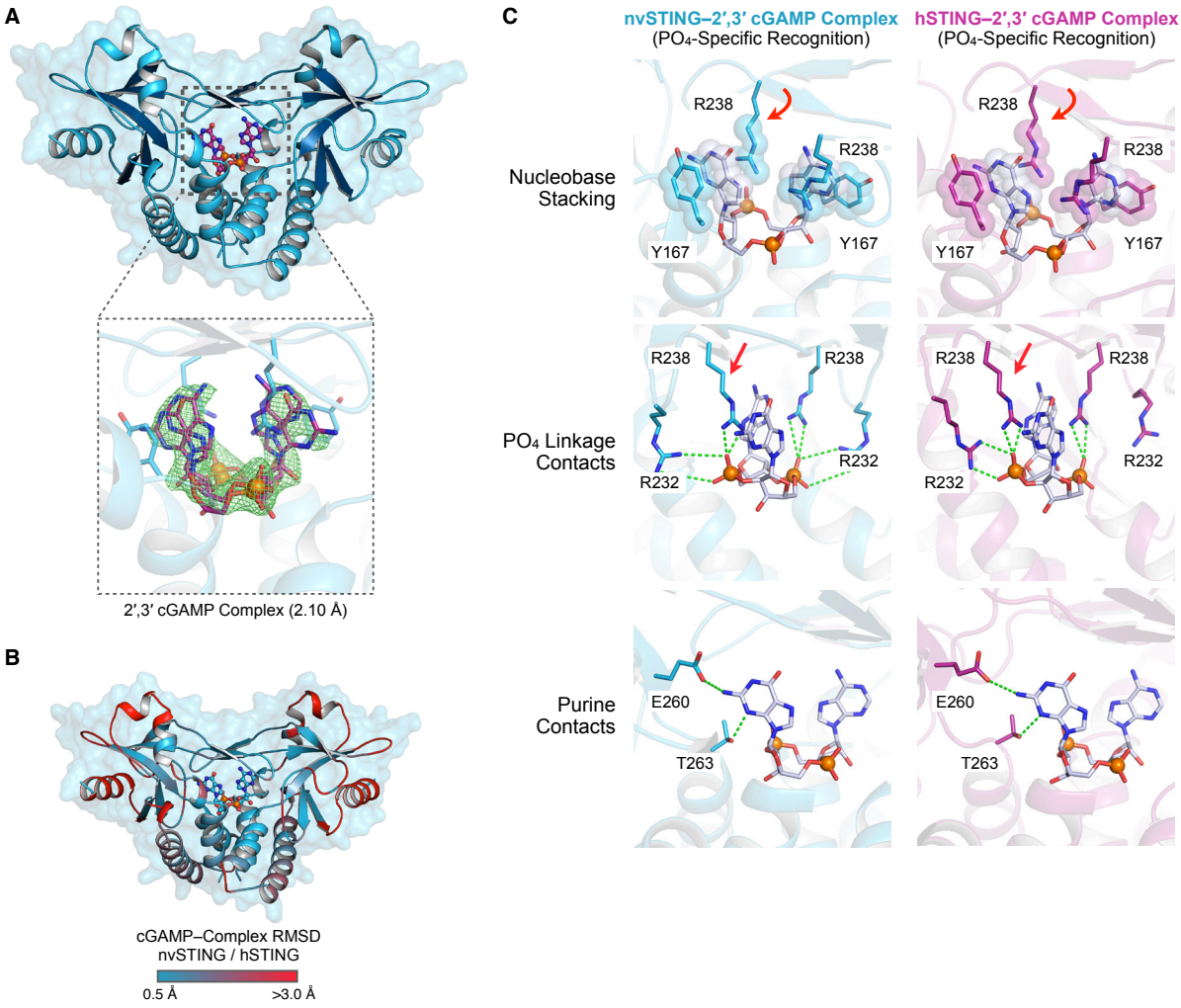

Figure S5. 2′,3′ cGAMP Traps an Evolutionarily Conserved Structural Intermediate, Related to Figure 5
(A) Crystal structure of nvSTING in complex with 2′,3′ cGAMP. Zoomed-in cutaway includes simulated-annealing F_o-F_c omit map of ligand density contoured to 3.5 σ. (B) Crystal structure of nvSTING–2′,3′ cGAMP complex colored according to RMSD divergence with hSTING–2′,3′ cGAMP structure (PDB 4KSY). The monomer wing pitch and core ligand-interacting portion of the nvSTING structure is unchanged, while movements are only present in the outer regions of the protein structure away from the central ligand binding pocket. (C) Detailed STING–CDN interactions in nvSTING–2′,3′ cGAMP (blue) and hSTING–2′,3′ cGAMP (magenta) complexes as described in Results and Figure 4. When bound to 2′,3′ cGAMP, nvSTING and hSTING each support phosphodiester-linkage contacts, indicating that 2′,3′ cGAMP traps an evolutionarily conserved intermediate irrespective of STING allele diversity. For clarity, nvSTING amino acids are numbered according to hSTING sequence.

Movie S1. Morph of STING Conformations Trapped by 2′,3′ and 3′,3′ CDN Binding, Related to Figure 6

Table S1. STING–CDN ITC Statistics

Table S1. ITC Parameters of nvSTING–CDN Complex Formation, Related to Figures 3, 5, and S5

Ligand	Protein (μM)	Replicates	K_D (nM)	ΔH (kcal mol^{-1})	ΔS (kcal mol^{-1} K^{-1})	n
nvSTING						
3′,3′ cGAMP	100	3	50 ± 4	−11.89 ± 1.09	−6.47 ± 3.83	0.57 ± 0.03
3′,3′ cGG	15	5	15 ± 6	−12.60 ± 0.92	−6.36 ± 3.49	0.46 ± 0.09
3′,3′ cAA	100	3	1,454 ± 141	−9.85 ± 0.41	−6.20 ± 1.07	0.29 ± 0.06
2′,3′ cGAMP	100	3	< 1	−4.53 ± 0.09	ND	0.45 ± 0.03
nvSTING (F236K)						
3′,3′ cGG	15	1	>500	ND	ND	ND
2′,3′ cGAMP	15	3	52 ± 25	−12,756 ± 907	−9.24 ± 3.69	0.51 ± 0.06

Supplemental Experimental Procedures

STING Allele Identification

STING orthologs were identified by a DELTA-BLAST (http://blast.ncbi.nlm.nih.gov/) query using mouse or human STING as input. High quality hits were aligned and used to construct a profile hidden Markov model using HMMER (http://hmmer.janelia.org) (Finn et al., 2011). The model was then used to search published animal genomes.

STING Allele Cloning and Protein Purification

Recombinant STING proteins were expressed and purified according to previously developed conditions for purification of human cGAS (Kranzusch et al., 2014). Codon-optimized sequence corresponding nvSTING (Genbank protein accession XP_001627385) was cloned from synthetic DNA oligos (IDT) into a modified pcDNA vector (Invitrogen) with a Kozak start sequence using Gibson assembly according to manufacturer's protocols (NEB). The nvSTING CDN receptor domain N193–G377(C-terminus) was amplified by PCR and cloned into a modified pET vector to express an N-terminal 6× His (KSSHHHHHHGSS)-MBP-TEV fusion

protein in BL21-RIL DE3 *E. coli* cells co-transformed with a pRARE2 tRNA (Agilent) plasmid. *E. coli* was grown in 2×YT media at 37°C to an OD_{600} of ~0.5 before being cooled at 4°C for 15 min and then incubated for ~18 h at 16°C with 0.5 mM IPTG induction. Following a PBS wash, cell pellets were lysed by sonication in lysis buffer (20 mM HEPES-KOH [pH 7.5], 400 mM NaCl, 10% glycerol, 30 mM imidazole, 1 mM TCEP) in the presence of EDTA-free Complete Protease Inhibitor (Roche). Recombinant STING protein was purified from clarified lysate by binding Ni-NTA agarose (QIAGEN). Resin was washed with lysis buffer supplemented to 1 mM NaCl, and eluted by gravity-flow chromatography at 4°C using lysis buffer supplemented to 300 mM imidazole. Recovered protein in elution buffer was diluted to 50 mM imidazole and 5% glycerol prior to concentration to ~80 mg ml^{-1} and digestion with Tobacco Etch Virus protease for ~12 h at 4°C. Homodimer STING was separated from the digested MBP tag by diluting with gel-filtration buffer (20 mM HEPES-KOH [pH 7.5], 250 mM KCl, 1 mM TCEP) and passing over a 5 ml Ni-NTA column (QIAGEN) connected in line with a 5 ml MBP-Trap column (GE Life Sciences) and further purified by size-exclusion chromatography on a Superdex 75 16/60 column. Final purified nvSTING was concentrate to ~40 mg ml^{-1}, used immediately for crystallography or flash frozen in liquid nitrogen for storage at −80°C and biochemical experiments. Selenomethionine-substituted nvSTING protein was prepared as previously described (Kranzusch et al., 2014). All animal STING alleles were cloned and expressed using analogous conditions. However for initial EMSA experiments, recombinant STING proteins from *X. tropicalis*, *D. rerio*, *D. melanogaster*, and *N. vitripennis* were expressed and purified with an amino terminal SUMO tag rather than a MBP tag, and recombinant STING proteins from *N. vectensis*, *S. harrisii*, *C. teleta*, *C. gigas*, *B. mori*, *B. terrestris*, and *M. musculus* were expressed without any solubility tag. Recombinant Vibrio DncV, human cGAS, nv-cGAS and nv-A7S0T1.1 synthases were purified and assayed for *in vitro* CDN-synthase activity according to previously published methods (Kranzusch et al., 2014).

STING–CDN Complex Gel Shift Assay

Radiolabelled cyclic dinucleotides were synthesized by incubating ~100 nM of α-^{32}P-ATP and/or α-^{32}P-GTP with 5 μM cold NTP and ~10 μM of the respective synthase: human cGAS 2′,3′ cGAMP synthase (Kranzusch et al., 2013; Schoggins et al., 2011), *Vibrio cholerae* DncV 3′,3′ cGAMP synthase (Davies et al., 2012; Kranzusch et al., 2014), *Pseudomonas aeruginosa* WspR* (D70E constitutively active mutant) 3′,3′ cGG synthase (Diner et al., 2013; Simm et al., 2009), *Bacillus subtilis* DisA 3′,3′ cAA synthase (Witte et al., 2008). Reactions were performed in 40 mM Tris-HCl (pH 7.5), 100 mM NaCl, 10 mM $MgCl_2$ and incubated at 37°C for 1–2 h. Human cGAS reactions were additionally supplemented with herring testes DNA.

Reactions were subsequently treated with 5 U of alkaline phosphatase (NEB) for 1 hour at 37°C. Following incubation, confirmation of cyclic dinucleotide synthesis was evaluated by thin-layer chromatography. Briefly, a 0.5 μl aliquot was spotted onto a Millipore TLC PEI cellulose F plate and placed into a glass chamber with a 1.5 M KH_2PO_4 (pH ~3.9) mobile phase. Following the appropriate amount of capillary action, the plates were removed, dried at 80°C for 10 minutes, and imaged in a phosphor cassette.

Reactions were then extracted with a phenol/chloroform/isoamyl alcohol mixture. The aqueous layer (top layer) was separated, mixed with 2.5 fold (v/v) ethanol, and evaporated to dryness using a Savant Speed Vac system. Radiolabelled cyclic dinucleotide stocks were typically re-suspended in 20 μl of water.

Approximately 10–100 μM of STING was used for each binding experiment. For binding experiments, purified STING proteins in ~200 mM KCl were diluted with binding buffer of 50 mM Tris-HCl (pH 7.5), 5 mM KCl, 10 mM $MgCl_2$, and 10% glycerol before adding CDN and incubating for 1 h on ice. All STING proteins were also independently incubated with radiolabelled phosphate to serve as a negative control. A loading dye was applied to each

sample and then immediately loaded onto a 6% acrylamide:bisacrylamide native gel (28:1). The gel was run in the cold room (4°C) for 90 minutes at 12 V. The gel was then dried for 2 hours at 60°C and imaged in a phosphor cassette.

STING–CDN ITC Analysis

All ITC measurements were performed on a MicroCal Auto-iTC200 (GE Healthcare). Experiments were conducted at 25°C using a degassed buffer comprised of 20 mM HEPES-KOH (pH 7.5), 250 mM KCl, 1 mM TCEP. Protein concentrations are shown in Table S2. All data fitting and analysis was done using Origin.

Crystallization and Structure Determination

nvSTING was crystallized in *apo* form or in complex with CDN ligands at 18°C by hanging drop vapor diffusion. Purified nvSTING CDN receptor domain was diluted on ice to 10 mg ml^{-1} in the presence of chemically synthesized 3′,3′ or 2′,3′ CDN ligands (BioLog). Following a 30 min incubation, 400 nl hanging drops were set at a 1:1 ratio over 70 µl of reservoir using a Mosquito robotics platform (TTP Labtech). Three sets of optimized crystallization conditions were obtained for independent nvSTING crystal forms: 200 mM $CaCl_2$, 100 mM HEPES-KOH pH 7.5, 28% PEG-400 (nvSTING *apo* “unrotated” *P* 2_1 2_1 2_1 crystals); 1.8 M ammonium citrate pH 7.0 (nvSTING–3′,3′ CDN and nvSTING *apo* “rotated” *P* 3_1 crystals); 500 mM $LiSO_4$, 2% PEG-8000 over a range of pH from ~4–7 (nvSTING–2′,3′ cGAMP *P* 2_1 2_1 2_1 crystals). nvSTING *apo* “unrotated” crystals grown in 28% PEG-400 conditions were harvested using reservoir solution supplemented with 15% ethylene glycol as a cryo-protectant prior to flash-freezing by submersion in liquid nitrogen. CDN bound nvSTING crystals were exquisitely sensitive and could only be harvested with oil as a cryoprotectant. Briefly, crystal drops were covered with a layer of saturated paratone-N or NVH oil (Hampton) and crystals were transferred from the drop into overlaying oil emersion using a Kozak cat whisker. The cat whisker was then used to gently

clean away excess mother liquor solution prior to harvesting the oil-submerged crystal with a nylon loop and flash-freezing in liquid nitrogen. X-ray diffraction data were collected under cryogenic conditions at the Lawrence Berkeley National Laboratory Advanced Light Source (Beamline 8.3.1).

Data were processed with XDS and AIMLESS (Kabsch, 2010) using the SSRL *autoxds* script (A. Gonzalez, Stanford SSRL). Indexed 3′,3′ CDN-bound crystals belonged to the trigonal spacegroup *P* 3_1, and *apo* or 2′,3′ cGAMP-bound crystals belonged to two different crystal forms in the orthorhombic spacegroup *P* 2_1 2_1 2_1. All crystals contained two copies of nvSTING CDN receptor domain in the asymmetric unit. Experimental phase information was determined using data from a single large nvSTING–3′,3′ cGG crystal collected at peak selenium absorbance energy and truncated to ~2.4 Å with strong anomalous signal to ~2.5 Å. Eight sites were identified with HySS in PHENIX (Adams et al., 2010), and an initial map was calculated using SOLVE/RESOLVE (Terwilliger, 1999) concurrent with phase extension to a native nvSTING–3′,3′ cGG data set processed to 1.84 Å. Initial maps displayed clear unbiased density for two nvSTING monomers and a central bound ligand, and model building was completed in Coot (Emsley and Cowtan, 2004) prior to refinement with PHENIX. Following completion of nvSTING–3′,3′ cGG model building, a monomeric model of nvSTING was prepared by removing ligand, protein loops and the beta-strand lid domain and used as a search model to determine phases for the other 3′,3′ CDN datasets using molecular replacement. A molecular replacement solution of the alternative STING conformation in the nvSTING–2′,3′ cGAMP dataset required searching with a significantly truncated core nvSTING monomer domain and then manual placement and rebuilding of nvSTING monomers into the density. In all nvSTING structures, x-ray data for refinement were extended according to an I/σ resolution cutoff of ~1.5, or extended an additional ~0.2 Å as determined by CC* correlation and R_{pim} parameters where visual inspection of the resulting map warranted data extension (Karplus and Diederichs, 2012).

Cell-Based Interferon β Luciferase Assay

Full-length human and bacteria CDN synthases and a 3′,3′ cGAMP phosphodiesterase were amplified from genomic DNA and cloned into pcDNA vectors (Invitrogen) or derived as following: human cGAS 2′,3′ cGAMP synthase (Kranzusch et al., 2013; Schoggins et al., 2011), *Vibrio cholerae* DncV 3′,3′ cGAMP synthase (Davies et al., 2012; Kranzusch et al., 2014), *Pseudomonas aeruginosa* WspR* (D70E constitutively active mutant) 3′,3′ cGG synthase (Diner et al., 2013; Simm et al., 2009), *Bacillus subtilis* DisA 3′,3′ cAA synthase (Witte et al., 2008), *Vibrio cholerae* 3′,3′ cGAMP phosphodiesterase (Gao et al., 2015). Bacterial genomic DNA was a kind gift from Dan Portnoy (University of California, Berkeley) and John Mekalanos (Harvard Medical School).

Synthase assays, and the *N. vectensis* screen for cGAS-like enzymes, were conducted in 293T human kidney cells as previously described (Kranzusch et al., 2014). Briefly, 293T cells at ~80% confluency were transfected using Lipofectamine 2000 (Invitrogen) in a 96-well format with the following plasmids: control Renilla luciferase reporter (2 ng), interferon β promoter driven Firefly luciferase reporter (20 ng), hSTING wt R232 (wild-type allele: R71, G230, R232, R293) or hSTING R232H plasmid (15 ng), and a CDN synthase plasmid (20–150 ng) as indicated (Figures 2 and 5). In Figure 2A and 2B, synthases are titrated from 0.1–50 ng (human cGAS, Pa WspR* and Bs DisA) or 10–150 ng (Vc DncV and nv-cGAS [nv-A7SFB5.1]). In Figure 2C, synthases are used at 20 ng (human cGAS, Pa WspR* and Bs DisA) or 150 ng (Vc DncV and nv-cGAS [nv-A7SFB5.1]). In Figure 2D, phosphodiesterase experiments were conducted at a 3:1 (phosphodiesterase 150 ng, synthase 50 ng) ratio as previously optimized (Gao et al., 2015). At 24 h post-transfection, Renilla and Firefly Dual-Luciferase values were assayed according to manufacture's protocols (Promega) using a Veritas Microplate Luminometer (Turner Biosystems) as previously described (Lee et al., 2015). Data were combined from multiple experiments and analyzed by an unpaired, two-tailed t test in Prism.

Supplemental References

Adams, P.D., Afonine, P.V., Bunkoczi, G., Chen, V.B., Davis, I.W., Echols, N., Headd, J.J., Hung, L.W., Kapral, G.J., Grosse-Kunstleve, R.W.*, et al.* (2010). PHENIX: a comprehensive Python-based system for macromolecular structure solution. Acta crystallographica Section D, Biological crystallography *66*, 213-221.

Chen, V.B., Arendall, W.B., 3rd, Headd, J.J., Keedy, D.A., Immormino, R.M., Kapral, G.J., Murray, L.W., Richardson, J.S., and Richardson, D.C. (2010). MolProbity: all-atom structure validation for macromolecular crystallography. Acta crystallographica Section D, Biological crystallography *66*, 12-21.

Davies, B.W., Bogard, R.W., Young, T.S., and Mekalanos, J.J. (2012). Coordinated regulation of accessory genetic elements produces cyclic di-nucleotides for V. cholerae virulence. Cell *149*, 358-370.

Diner, E.J., Burdette, D.L., Wilson, S.C., Monroe, K.M., Kellenberger, C.A., Hyodo, M., Hayakawa, Y., Hammond, M.C., and Vance, R.E. (2013). The innate immune DNA sensor cGAS produces a noncanonical cyclic dinucleotide that activates human STING. Cell reports *3*, 1355-1361.

Emsley, P., and Cowtan, K. (2004). Coot: model-building tools for molecular graphics. Acta crystallographica Section D, Biological crystallography *60*, 2126-2132.

Finn, R.D., Clements, J., and Eddy, S.R. (2011). HMMER web server: interactive sequence similarity searching. Nucleic acids research *39*, W29-37.

Gao, J., Tao, J., Liang, W., Zhao, M., Du, X., Cui, S., Duan, H., Kan, B., Su, X., and Jiang, Z. (2015). Identification and characterization of phosphodiesterases that specifically degrade 3'3'-cyclic GMP-AMP. Cell research.

Kabsch, W. (2010). Xds. Acta crystallographica Section D, Biological crystallography *66*, 125-132.

Karplus, P.A., and Diederichs, K. (2012). Linking crystallographic model and data quality. Science *336*, 1030-1033.

Kranzusch, P.J., Lee, A.S., Berger, J.M., and Doudna, J.A. (2013). Structure of human cGAS reveals a conserved family of second-messenger enzymes in innate immunity. Cell reports *3*, 1362-1368.

Kranzusch, P.J., Lee, A.S., Wilson, S.C., Solovykh, M.S., Vance, R.E., Berger, J.M., and Doudna, J.A. (2014). Structure-guided reprogramming of human cGAS dinucleotide linkage specificity. Cell *158*, 1011-1021.

Lee, A.S., Kranzusch, P.J., and Cate, J.H. (2015). eIF3 targets cell-proliferation messenger RNAs for translational activation or repression. Nature *522*, 111-114.

Schoggins, J.W., Wilson, S.J., Panis, M., Murphy, M.Y., Jones, C.T., Bieniasz, P., and Rice, C.M. (2011). A diverse range of gene products are effectors of the type I interferon antiviral response. Nature *472*, 481-485.

Simm, R., Remminghorst, U., Ahmad, I., Zakikhany, K., and Romling, U. (2009). A role for the EAL-like protein STM1344 in regulation of CsgD expression and motility in Salmonella enterica serovar Typhimurium. Journal of bacteriology *191*, 3928-3937.

Sureka, K., Choi, P.H., Precit, M., Delince, M., Pensinger, D.A., Huynh, T.N., Jurado, A.R., Goo, Y.A., Sadilek, M., Iavarone, A.T.*, et al.* (2014). The cyclic dinucleotide c-di-AMP is an allosteric regulator of metabolic enzyme function. Cell *158*, 1389-1401.

Terwilliger, T.C. (1999). Reciprocal-space solvent flattening. Acta crystallographica Section D, Biological crystallography *55*, 1863-1871.

Weiss, M.S. (2001). Global indicators of X-ray data quality. J Appl Crystallogr *34*, 130-135.

Witte, G., Hartung, S., Buttner, K., and Hopfner, K.P. (2008). Structural biochemistry of a bacterial checkpoint protein reveals diadenylate cyclase activity regulated by DNA recombination intermediates. Molecular cell *30*, 167-178.